Article

Not peer-reviewed version

# Eddy Covariance Measurements Reveal Enhanced $CO_2$ Flux and Evapotranspiration Under Simulated Agrivoltaics Shading in Deciduous Orchards

Dafna Eliyahou * and Giora Rytwo

Posted Date: 27 May 2026

doi: 10.20944/preprints202605.1890.v1

Keywords: eddy covariance; APV; $CO_2$ flux; ET; shading; orchard; semi-arid climate

 doi:10.20944/preprints202605.1890.v1



*Article*

# Eddy Covariance Measurements Reveal Enhanced $CO_2$ Flux and Evapotranspiration Under Simulated Agrivoltaics Shading in Deciduous Orchards

**Dafna Eliyahou [1,2,3,*] and Giora Rytwo [1,2]**

[1] Environmental Physical Chemistry Laboratory, MIGAL-Galilee Research Institute, P.O. Box 813, Kiryat Shmona 1101600, Northern District, Israel

[2] Faculty of Sciences and Technology, Tel-Hai University of Kiryat Shmona in the Galilee, 1220800 Northern District, Israel

[3] Dr. Moses Strauss Department of Marine Geosciences, Leon H. Charney School of Marine Sciences. University of Haifa, Mount Carmel, Haifa 31905, Israel

* Correspondence: dafna.eliyahou@gmail.com

**Highlights:**

- APV shading alters orchard microclimate & fluxes.
- Higher $CO_2$ uptake & ET in shaded areas.
- Shading reduces stress, improves photosynthesis.
- Shading enhances water use efficiency in semi-arid zones.
- Novel EC-APV study in deciduous orchards.

**Abstract**

Agrivoltaics (APV) systems, integrating solar energy generation with agriculture, offer a promising solution for optimizing land use facing a rising energy demand and climate change concerns. However, the impact of APV induced shading on orchards micrometeorology and physiology is not fully understood. This study investigated the effects of simulated APV shading on sensible heat flux, temperature, humidity, wind, $CO_2$ flux, and evapotranspiration (ET) in deciduous plum and nectarine orchards in northern Israel. Using the eddy covariance (EC) method, we measured $CO_2$ and water vapor fluxes in adjacent shaded and unshaded (referred to as 'paneled' and 'sunlit') sections. Principal component analysis (PCA) and linear regression were employed to analyze the relationships between meteorological variables and the measured fluxes. Results showed significantly higher rates of $CO_2$ flux (absorption) and ET in the paneled sections compared to sunlit sections, particularly during summer peak radiation hours. These findings suggest that partial shading moderates environmental stress (excessive heat, high vapor pressure deficit), improving stomatal function, enhancing photosynthesis, and potentially promoting water use efficiency. This research integrates the EC method with APV system analyses in orchards, providing novel insights into the dynamic interactions under shading and highlighting the potential of APV to enhance agricultural sustainability in semi-arid climates.

**Keywords:** eddy covariance; APV; $CO_2$ flux; ET; shading; orchard; semi-arid climate

## 1. Introduction

The combination of projected global population growth, expected to reach 9.7 billion by 2050 (United Nations, 2021), and a near-doubling of energy demand over the coming decades (Energy Information Administration (EIA), 2016; Lewis and Nocera, 2006) presents profound challenges for sustainable development. Addressing this escalating energy demand while simultaneously mitigating climate change, as targeted by international agreements like the United Nations Paris

 doi:10.20944/preprints202605.1890.v1



Agreement, 2015, aiming to limit global warming, necessitates a significant shift towards clean, renewable energy sources. Many nations have set progressive renewable energy goals; for instance, the EU aims for 32% renewable energy production by 2030 (EU Commission, 2011).

Among renewable options, solar energy is the most abundant globally and has become increasingly cost-effective, especially for large, open-area PV installations (IRENA, 2023; Rogner et al., 2012). Indeed, PV and onshore wind are now cost-competitive with fossil fuels in many regions (IRENA, 2019). However, the rapid expansion required for solar energy leads to significant land-use challenges. Unlike fossil fuels, whose geographical footprint is largely confined to extraction points, renewable energy generation often requires extensive land allocation, creating potential conflicts with other essential land uses.

Land scarcity further complicates this transition. Approximately 35% of the global land surface is currently dedicated to agriculture (Nonhebel, 2005), and food production must increase substantially to meet the demands of a growing and urbanizing population (Tilman et al., 2011). Simultaneously, land availability is under pressure from soil degradation and urban expansion (UNCCD, 2017). This intensifies the competition for land between renewable energy expansion, agriculture, and environmental conservation.

### *1.1. Agrivoltaics as a Sustainable Land-Use Solution*

Agrivoltaics, also known as agrophotovoltaics, emerges as a potential solution to this land-use dilemma by integrating PV energy generation with agricultural activities on the same land. First proposed conceptually in the early 1980s (Goetzberger and Zastrow, 1982) and formally studied later (Dupraz et al., 2011), APV aims to optimize overall land productivity. This dual-use approach can modify the microclimate beneath the panels, potentially reducing crop heat stress and improving soil moisture retention, which may enhance productivity, particularly in resource-limited environments (Weselek et al., 2021). Studies suggest APV can significantly increase land productivity values (Dupraz et al., 2011; Elamri et al., 2018; Valle et al., 2017) and the economic value of land use (Dinesh and Pearce, 2016).

APV systems hold particular promise for mediterranean, semi-arid, and arid regions, where crops often face challenges from high solar radiation and water scarcity (Marrou et al., 2013a). Evidence suggests that water use efficiency can be improved under PV panels (Elamri et al., 2018; Hassanpour et al., 2018; Marrou et al., 2013a), a critical benefit as irrigation demands is expected to rise under future climate scenarios. Furthermore, the reduction in solar radiation under the panels may benefit crops sensitive to intense sunlight (Hassanpour et al., 2018; Ravi et al., 2016). For example, dramatic increases in biomass and water efficiency were observed under PV canopies in a semi-arid site in Oregon, USA (Hassanpour et al., 2018), and studies in Germany found APV crop yields significantly exceeded reference fields during dry, hot years (Trommsdorff et al., 2021). These findings suggest APV could be highly beneficial in climates like Israel's.

### *1.2. Impacts of APV Shading on Orchard Productivity*

However, the impact of shading, a key feature of APV systems, on crop productivity requires careful consideration, especially for perennial systems like orchards. Light availability is often the most critical factor influencing yield under APV (Marrou et al., 2013b; Trommsdorff et al., 2021). While solar radiation drives essential processes like photosynthesis and fruit development, excessive radiation can induce heat stress and cause fruit damage like sunburn (Glenn, 2009; Middleton and McWaters, 2002). Moderate shading (from netting or APV panels) can mitigate these stresses, but insufficient light can impair carbohydrate supply to fruits (Grappadelli et al., 1994). Plants have a light saturation point for photosynthesis; excess light beyond this point primarily increases water loss through transpiration (Kramer and Boyer, 1995; Gates, 1968). APV systems might optimize this balance, improve water availability and protect plants from intense sunlight (Barron-Gafford et al., 2019; Elamri et al., 2018), potentially favouring plants with high photosynthetic rates (Seidlova et al., 2009). Positive yield impacts under APV have been reported for various crops like grapes, lettuce,

 doi:10.20944/preprints202605.1890.v1



and tomatoes (Barron-Gafford et al., 2019; Elamri et al., 2018; Marrou et al., 2013b). However, the shading under APV is typically non-uniform and dynamic, varying with panel design, orientation, and solar position (Beck et al., 2012; Dupraz et al., 2011), and its specific effects on orchard trees remain less explored.

### *1.3. Agrometeorological Framework and Measurement Techniques*

Understanding these effects requires considering the principles of agrometeorology, the study of interactions between weather, climate, and agriculture. Key variables like air temperature, humidity, radiation, and wind speed operating within the atmospheric boundary layer govern crop growth, development, and physiological processes (Boote and Loomis, 1991; Hubbard and Hollinger, 2005; Lehner and Rotach, 2018; Allen et al., 1998; Teixeira et al., 2016). These variables directly influence ET, the combined water loss from soil evaporation and plant transpiration, a critical factor in water management (Allen et al., 1998). Transpiration, the dominant component of ET in vegetated areas, is intrinsically linked to photosynthesis ($CO_2$ uptake) through stomatal pores on leaves. Stomata regulate gas exchange, but their opening for $CO_2$ inevitably allows water vapor to escape. Stomatal aperture is dynamically controlled by environmental factors including photosynthetically active radiation (PAR), T, vapor-pressure deficit (VPD), and leaf water potential (LWP) (Jarvis, 1976). Environmental stresses like high T or low LWP can trigger stomatal closure, limiting both water loss and $CO_2$ uptake. Understanding these biophysical controls is essential for predicting plant responses to altered microclimates, such as those under APV shading, and their implications for carbon and water cycles (Farquhar et al., 1993; Foley et al., 1994; Prentice et al., 2000; Sellers et al., 1997).

These gas exchange processes are fundamentally linked to the surface energy balance. Net radiation (Rn), the balance between incoming and outgoing shortwave and longwave radiation, is the primary energy input driving surface processes. This available energy is partitioned primarily into sensible heat flux (H, warming the air), latent heat flux (LE, energy used for ET), and ground heat flux (G, warming the soil) (Baldocchi et al., 2000; Steiner and Hatfield, 2008; Testi et al., 2004; Venkatram and Schulte, 2018). APV systems likely influence the partitioning of Rn into H and LE, thereby affecting both the microclimate (T, humidity) and the rates of ET and photosynthesis.

To directly measure these surface-atmosphere exchange processes ($CO_2$ flux, ET/LE, H), the EC method is widely recognized as a standard and accurate micrometeorological technique (Burba, 2013; Foken et al., 2012; Mahrer and Rytwo, 1991; Rytwo and Eliyahou, 2023). It measures the covariance between turbulent fluctuations in vertical wind speed and the concentration of the scalar of interest (as $CO_2$, water vapor, T). While APV systems have been studied for impacts on yield and microclimate point measurements, and the EC method is well-established for ecosystem-scale flux quantification, there is limited research combining these approaches, particularly in complex orchard environments.

### *1.4. Research Gap, Objectives, and Hypothesis*

This study aims to bridge this gap by employing the EC technique to investigate the effects of simulated APV shading on $CO_2$ flux and ET in deciduous orchards within a Mediterranean/semi-arid climate. Our central hypothesis is that the partial shading imposed by simulated APV panels will alter the orchard microclimate and, consequently, the measured fluxes of $CO_2$ and water vapor compared to adjacent unshaded areas. By analyzing these flux dynamics in relation to key meteorological drivers, we seek to provide novel insights into the interactions between APV shading, orchard physiology, and the atmospheric environment, contributing to a better understanding of APV's potential for sustainable agriculture and renewable energy integration.

 doi:10.20944/preprints202605.1890.v1



## 2. Methods

### *2.1. Study Sites*

The research was conducted at two commercial deciduous fruit orchards located in the Upper Galilee region of Northern Israel; an area characterized by a Mediterranean climate transitioning to semi-arid conditions. Both sites were maintained under standard agricultural practices, including daily drip irrigation to ensure well-watered conditions throughout the experimental periods.

#### 2.1.1. Plum Orchard

The first site was a plum orchard located in Kibbutz Ayelet Ha'Shahar (latitude 33.015°N, longitude 35.58°E, elevation 173 m above sea level), covering an area of 42,601 m². Trees were planted at 4.5 m spacing between rows and 2.0 m between trees, resulting in an estimated 4,733 trees of approximately 2.5 meters height. To simulate the shading effect of an APV system, 2-meter-wide straps of tarpaulin were deployed above three successive tree rows at a height of approximately 3 meters, positioned in the mid-interval between tree lines, creating a 394 m² shaded polygon, representing 0.93 % of the plot surface. The 3.5-meter-high EC station alternated between the shaded and sunlit sections (Figure 1). Measurements at this site were conducted during the summer and autumn of 2021, from July 2nd to December 11th.


**Figure 1.** Study sites and instrumentation. Maps, aerial views, and photographs of the eddy covariance station are shown for the two experimental orchards: (A) the plum orchard at Ayelet Ha'Shahar and (B) the nectarine orchard at Yiftah.

#### 2.1.2. Nectarine Orchard

The second site was a nectarine orchard in Kibbutz Yiftah (latitude 33.12°N, longitude 35.54°E, elevation 410 m above sea level). This orchard covered an area of 32,504 m². Trees were planted with 4.0 m between rows and 2.5 m between trees, totaling approximately 3,250 trees. The simulated shading setup here consisted of six successive rows of tarpaulin, each 45 meters long and 3 meters wide, installed at a height of 4 meters, forming a combined 1,075 m² shaded area, amounting to 3.31 % of the plot. The 4.5-meter-high EC station alternated between the shaded and sunlit sections (Figure 1). Measurements at the Yiftah site were carried out during the summer and autumn of 2022, from July 7th to December 1st.

At both locations, a single EC system was employed and alternated between the paneled (shaded) and sunlit sections approximately every 10-15 days to capture data under both treatment conditions.

 doi:10.20944/preprints202605.1890.v1



*2.2. Eddy Covariance (EC) Method and System*

2.2.1. EC Principles

The EC technique is a fundamental micrometeorological method used to directly measure the exchange rates (fluxes) of mass (like $CO_2$, $H_2O$) and energy (like sensible heat) between the Earth's surface and the overlying atmosphere. It is considered one of the most accurate approaches for quantifying these fluxes and has been widely applied across various ecosystems, including agricultural landscapes, since the early 1990s (Burba, 2013; Foken et al., 2012; Mahrer and Rytwo, 1991; Rytwo and Eliyahou, 2023).

The method relies on the principle that transport in the atmospheric boundary layer is dominated by turbulence, which consists of rotating air parcels or "eddies" moving three-dimensionally (Foken et al., 2012; Mahrer and Rytwo, 1991; Venkatram and Schulte, 2018). By measuring the instantaneous fluctuations in vertical wind speed and the scalar quantity of interest at high frequency, the flux can be calculated as the covariance between these fluctuations, averaged over a suitable period. Under assumptions of horizontal homogeneity and stationarity, where mean vertical flow and density fluctuations are negligible, the flux is typically calculated as:

$$F = \overline{\rho_a}\,\overline{w' x_s'} \quad (1)$$

Equation (1) is a classic formula for the eddy flux of any gas of interest. The product of mean air density ($\overline{\varrho_a}$, kg m$^{-3}$), and the mean covariance between instantaneous deviations in vertical wind speed ($\overline{w'}$, m s$^{-1}$) and mixing ratio ($\overline{x_s'}$, mol$_s$ mol$_d^{-1}$) of substance 's' (Gu et al., 2012). The EC method requires instruments capable of high-frequency measurements, assumes the measurement footprint adequately represents the surface of interest, and relies on sufficient turbulence (Burba, 2013). These assumptions must be considered during site selection and data analyses, especially in complex terrains like orchards.

2.2.2. Instrumentation

The EC system deployed in this study comprised of two sensors:

1. A 3D ultrasonic anemometer (WindMaster PRO 32 Hz, Gill Instruments Ltd.,) to measure the three orthogonal components of wind speed (u, v, w) and the sonic temperature ($T_s$) at high frequency. The sonic anemometer calculates wind speed based on the transit time of ultrasonic pulses between transducer pairs. $T_s$ (in °C) is derived from the speed of sound (c) using the relationship:

$$T_s = \frac{c^2}{y_d R_d} - 273.15 \quad (2)$$

Where $R_d$ is the gas constant for dry air and $y_d$ is the ratio of specific heat of moist air at constant pressure to that at constant volume.

2. An open-path, non-dispersive infrared (NDIR) gas analyzer (LI-7500 DS, LI-COR Inc.) to measure fluctuations in the molar densities of $CO_2$ and $H_2O$ vapor in the air path between the instrument's source and detector. The NDIR analyzer operates by measuring the absorption of infrared radiation at specific wavelengths characteristic of $CO_2$ (approx. 4.26 μm) and H2O (approx. 2.59 μm).

The sensors were mounted on an adjustable-height tower, positioned at 3.5 m in Ayelet Ha'Shahar and 4.5 m in Yiftah, above the estimated zero-plane displacement height, oriented to minimize flow distortion from the tower structure relative to prevailing winds. Data from both sensors were synchronized and logged at a frequency of 10 Hz using a SmartFlux3 System datalogger (LI-COR Inc.). These high-frequency data were processed in real-time and also stored for post-processing to compute 30-minute average fluxes and other meteorological parameters (such as friction velocity, H, LE, ET, momentum flux, T, relative humidity (RH), VPD, etc.

 doi:10.20944/preprints202605.1890.v1



*2.3. Data Processing and Analyses*

2.3.1. Flux Corrections and Quality Control

Raw 10 Hz data were processed into 30-minute flux averages using the EddyPro software following established protocols (Aubinet et al., 2012). Standard processing steps applied within EddyPro using default settings included spike detection and removal, coordinate rotation (tilt correction), spectral correction, Webb-Pearman-Leuning (WPL) correction

EddyPro also performs quality checks based on tests for stationarity and integral turbulence characteristics, flagging data that do not meet certain criteria. Only daytime data (identified by incoming radiation or daytime flag in EddyPro output) were used for subsequent analyses comparing photosynthetic activity and transpiration.

2.3.2. Footprint Analysis

The source area (footprint) represented by the EC systems was quantified with the two-dimensional Flux-Footprint Prediction (FFP) parameterization of Kljun et al. (2015) and compared with the classical rule-of-thumb that the footprint radius is ≈ 100 × measurement height (Leclerc & Thurtell 1990). The FFT model expresses the cross-wind-integrated footprint as a non-dimensional coordinate, $X^*$, where the peak of that function occurs at a universal value $X^*_{max} = 0.87$. In dimensional form the peak contribution distance ($x_{peak}$), the single most-influence contribution distance, is calculated from:

$$x_{peak} = 0.87 \cdot z_d \left(1 - \frac{z_d}{h}\right)^{-1} \cdot \frac{u^* \cdot lan\left(\frac{z_d}{z_0}\right)}{u^*} \quad (3)$$

The parameters used in Eq.3, specifically for the Ayelet Ha'Shahar and Yiftah sites, are summarized below (Table 1).

Under the above conditions, $x_{peak}$ was found to be $8 - 10\,m$. Cumulative distances enclosing 80% and 90% of the scalar flux, obtained from the lookup factors in Kljun et al. (2015), were $x_{80} \approx 60 - 70\,m$ and $x_{90} \approx 150 - 170\,m$, respectively.

For comparison, the rule-of-thumb gives radii of 350m for Ayelet Ha'Shahar and 450m for Yiftah, representing upper-bound fetches under weak turbulence.

It is important to note that the shaded zones were limited in area (394 m² at Ayelet Ha'Shahar and 1,075 m² at Yiftah). As the measurement footprints extend well beyond these areas, a significant portion of the measured fluxes originated from the adjacent sunlit canopy or from outside the experimental plots. Crucially, while the point of maximum flux density ($x_{peak} = 8 - 10m$) was located within the shaded strips at both sites, beyond this distance, 70-92% of the cumulative source area covered sunlit canopy. This mixing of footprints renders the reported treatment differences conservative, implying that the actual impact of shading on $CO_2$ and ET fluxes is likely greater than what was directly measured. This limitation is discussed further in Section 4.3.

**Table 1.** Footprint Analysis (FFP) Parameters and Values for both study sites.

| Parameter | Symbol | Description | Ayelet Ha'Shahar (Plum orchard) | Yiftah (Nectarine orchard) |
|---|---|---|---|---|
| Sensor Height | $z$ | Height of the Eddy Covariance (EC) sensor above the ground. | $3.5m$ | $4.5m$ |

 doi:10.20944/preprints202605.1890.v1



| | | | | |
|---|---|---|---|---|
| Canopy Height | $h_c$ | Estimated average height of the orchard canopy. | $2.5m$ | $3.5m$ |
| Friction Velocity | $u^*$ | Characteristic turbulent velocity, measured during midday, clear sky periods. | $0.50\ m\ s^{-1}$ | |
| Boundary Layer Height | $h$ | Assumed height of the atmospheric boundary layer under the specified conditions. | $1000m$ | |
| Displacement Height | $d$ | Effective height above ground where mean wind speed becomes zero, approximated as 0.7 times the canopy height ($\approx 0.7 \cdot h_c$). | $1.75m$ | $2.45m$ |
| Effective Height | $z_d$ | The effective height above the displacement level, the difference between the sensor height and the displacement height ($z - d$). | $1.75m$ | $2.05m$ |
| Roughness Length | $z_0$ | Height at which wind speed theoretically becomes zero, approximated as 0.1 times the canopy height ($\approx 0.1 \cdot h_c$) | $0.25m$ | $0.35m$ |

2.3.3. Principal Component Analysis (PCA)

Due to the inherent high correlation among meteorological variables influencing surface fluxes, standard regression techniques can be problematic. Therefore, PCA was employed as a dimensionality-reduction and correlation-elimination technique to analyze the relationships between the primary meteorological drivers and the measured fluxes ($CO_2$ and ET) (Abdi and Williams, 2010).

PCA transforms a set of possibly correlated variables into a set of linearly uncorrelated variables called principal components (PCs). The first few PCs capture the majority of the variance in the original dataset, allowing for a simplified representation of the underlying environmental gradients (Wold et al., 1987). PCA has been widely used in meteorological and environmental studies for pattern identification and data reduction (Jolliffe, 2002; Preisendorfer R. W., 1988).

For this study, PCA was performed using R software (version 4.2.1) on a subset of the data identified as having the most significant treatment differences: measurements collected during the summer season (; July 2nd – September 21st, 2021, for plums; July 7th – September 21st, 2022, for nectarines) between the hours of 8 AM and 5 PM. The input variables for the PCA were the key meteorological drivers measured or derived by the EC system: H, mean prevailing wind speed ($u_{rot}$ , derived from u and v components after rotation), VPD, and T.

Prior to PCA, these variables were standardized and centred to have a mean of zero and scaled (thus have a standard deviation of one), ensuring all variables contributed equally to the analyzis regardless of their original units or magnitudes. The PCA was computed from the covariance matrix of the standardized data. The resulting PCs are orthogonal linear combinations of the original standardized variables, ranked by the amount of variance they explain (eigenvalues).

2.3.4. Statistical Modelling

The first three or four PCs, which collectively explained >95% of the variance in the meteorological data at both sites, were retained for subsequent analyses. These PCs served as

 doi:10.20944/preprints202605.1890.v1



independent predictor variables in linear regression models built using JAMOVI statistical software (version 2.3). Separate models were constructed for $CO_2$ flux and ET as dependent variables. The models included the PCs as covariates and the treatment type ('Paneled' or 'Sunlit') as categorical factors to test for significant differences in fluxes between the shaded and unshaded sections, while accounting for the underlying meteorological variability captured by the PCs. Model assumptions, including normality of residuals, were checked. Significance was assessed at $p < 0.01$. To further visualize the relationships and treatment effects under varying conditions, scatter plots of fluxes versus key meteorological drivers (T, H), stratified by treatment, season, and levels of other variables (VPD, $u_{rot}$), were generated using the openair package in R.

## 3. Results

### *3.1. Plum Orchard (Ayelet Ha'Shahar)*

#### 3.1.1. Meteorological Context

During the summer daytime measurement (08:00-17:00), the paneled rows were characterised by a slightly higher VPD than the adjacent sunlit control. H showed no clear treatment effect under shade versus the sunlit rows. $u_{rot}$ was marginally lower beneath the paneled area than in the sunlit. Mean air T differed by < 0.5 K but was nonetheless significant.

**Table 2.** Statistical summary of mean, standard deviation, and statistical significance (p-value) for key meteorological variables in the plum orchard, comparing paneled and sunlit sections during summer daytime (N=1,128).

| **Meteorological Variable** | **Paneled Section (*Mean ± SD*)** | **Sunlit Section (*Mean ± SD*)** | ***p*-value** |
|---|---|---|---|
| Vapor-Pressure Deficit (VPD) (Pa) | 3302 ± 1002 | 3093 ± 927 | < 0.001 |
| Sensible Heat Flux (H) (W $m^{-2}$) | 168 ± 80 | 176 ± 70 | 0.099 |
| Prevailing Wind Speed ($u_{rot}$) (m $s^{-1}$) | 1.69 ± 0.83 | 2.06 ± 0.88 | < 0.001 |
| Air Temperature (T) (K) | 307.33 ± 2.82 | 306.85 ± 2.40 | 0.03 |

These modest yet significant micro-climatic contrasts, particularly the elevated VPD and slight cooling under shade, provide the immediate physical context for the flux responses discussed in the following sections.

#### 3.1.2. PCA

PCA was applied to the data from the plum orchard. The analysis included H, $u_{rot}$, VPD, and T. The first principal component (PC1) showed strong positive correlations with VPD and T, a negative correlation with H, and a less pronounced positive correlation with $u_{rot}$. PC2 was dominated by a positive correlation with $u_{rot}$ and negative correlations with H, VPD, and T, with H being the most significant among the latter. PC3 was primarily characterized by strong positive correlations with H and $u_{rot}$, with minimal influence from VPD and T. The first three principal components collectively explained 98.59% of the total variance in the dataset, indicating high accuracy in capturing data variability.

Linear regression models were used to describe the relationship between the above principal components and ET and $CO_2$ flux. Both models showed a significant relationship ($p < 0.001$) during the summer season (July 2nd - September 21st) between 8 AM and 5 PM. The PCs explained 34.57% of the variability in ET and 27.67% of the variability in $CO_2$ flux.

 doi:10.20944/preprints202605.1890.v1



3.1.3. Fluxes (Summer, 8 AM-5 PM)

$CO_2$ flux

$CO_2$ flux measurements during the summer (8 AM - 5 PM) revealed a significant difference between the paneled and sunlit sections, as detailed in Table 3. The paneled section exhibited significantly higher $CO_2$ absorption, indicating greater photosynthetic activity compared to the sunlit section. These results highlight the moderating effect of shading on carbon uptake during the peak measurement period.

**Table 3.** Statistical summary of mean, standard deviation, and statistical significance (F-statistic, p-value) for $CO_2$ flux and ET in the plum orchard, comparing paneled and sunlit sections during summer daytime.

| **Variable** | **Treatment** | ***Mean* ± *SD*** | **Statistical Comparison (*F*-statistic, *p*-value)** |
|---|---|---|---|
| $CO_2$ flux | Paneled | -7.757 ± 2.625 μmol $m^{-2}$ $s^{-1}$ | $F_{1,128}$=195.52, p<0.001 |
| | Sunlit | -6.081 ± 1.413 μmol $m^{-2}$ $s^{-1}$ | |
| ET | Paneled | 0.1433 ± 0.0579 mm $hr^{-1}$ | $F_{1,128}$=50.58, p<0.001 |
| | Sunlit | 0.1144 ± 0.0447 mm $hr^{-1}$ | |

The relationship between $CO_2$ flux and H was nonlinear in the paneled section, with higher absorption at moderate sensible heat levels (~150–300 W $m^{-2}$). The sunlit section showed a linear decrease in $CO_2$ absorption with increasing H, suggesting greater sensitivity to heat stress. There was no apparent correlation between wind speed and sensible heat or $CO_2$ fluxes in either section (Figure 2).

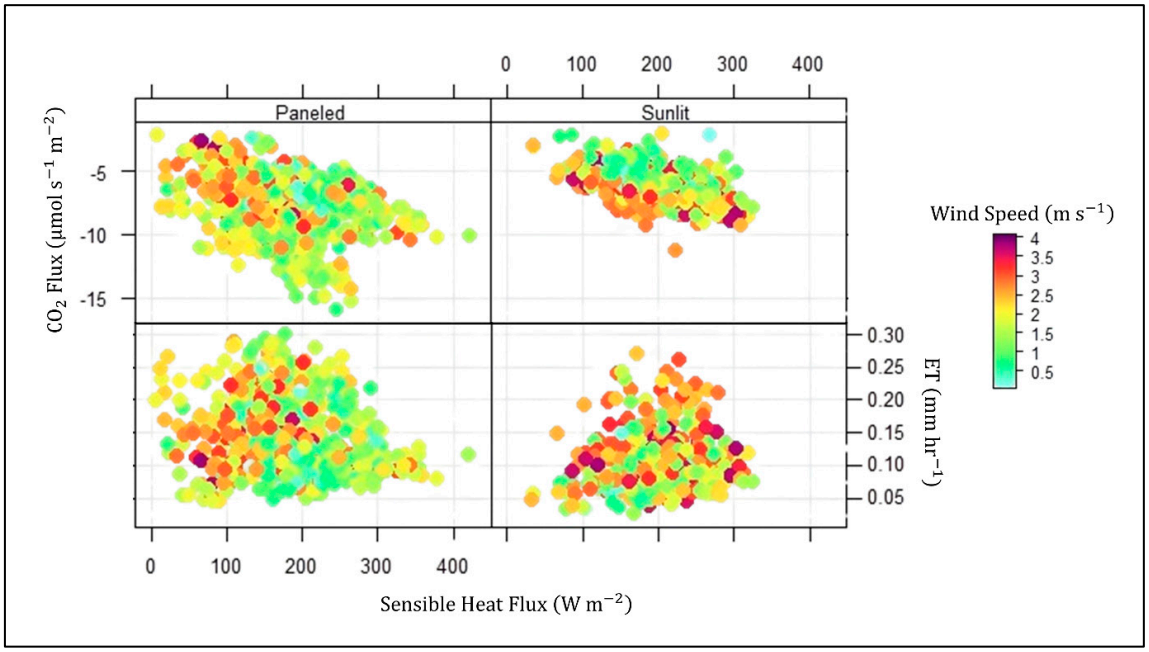


**Figure 2.** Relationship between $CO_2$ flux (top) and evapotranspiration (ET, bottom) versus sensible heat flux in the plum orchard. Data are shown for paneled (left) and sunlit (right) sections during summer daytime hours. Data points are colored according to prevailing wind speed.

 doi:10.20944/preprints202605.1890.v1



Regarding the relationship between $CO_2$ flux and T, the paneled section showed increased absorption up to ~308 K, after which it levelled off. Higher VPD levels in the paneled section maintained higher $CO_2$ absorption rates than in the sunlit section. The sunlit section exhibited a more moderate response, with $CO_2$ absorption declining as T increased, particularly under high VPD conditions (Figure 3).

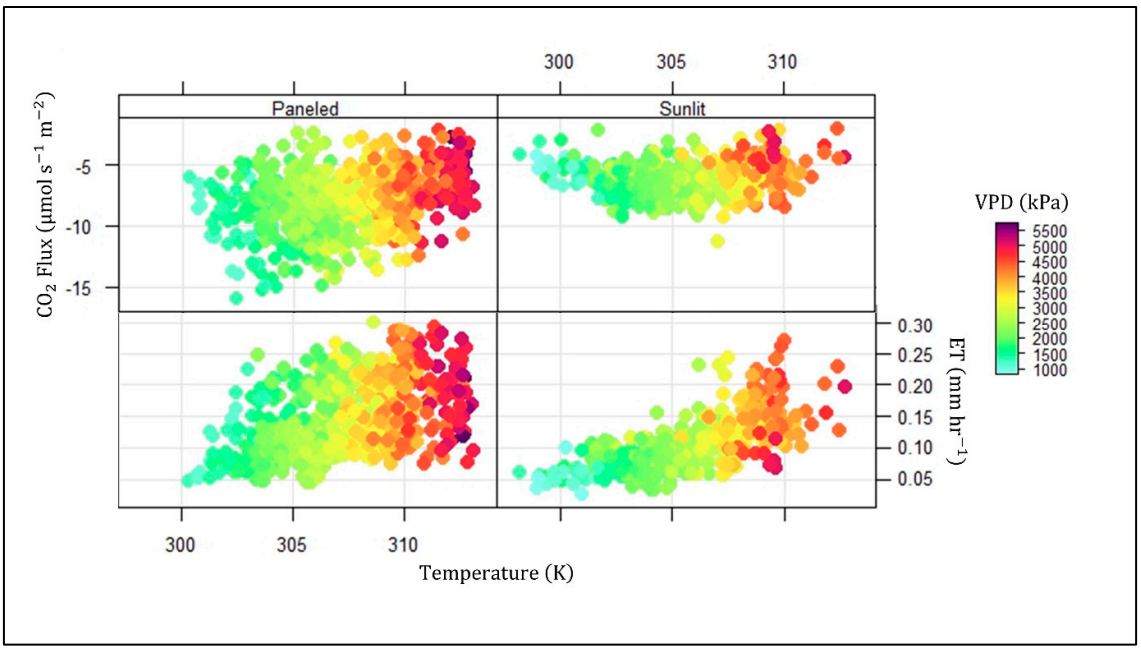


**Figure 3.** Relationship between $CO_2$ flux (top) and evapotranspiration (ET, bottom) versus temperature in the plum orchard. Data are shown for paneled (left) and sunlit (right) sections during summer daytime hours. Data points are colored according to vapor pressure deficit (VPD).

Evapotranspiration

ET rates also showed a statistically significant difference between the paneled and sunlit sections during summer (8 AM - 5 PM) (Table 3). The paneled section consistently exhibited higher mean ET rates compared to the sunlit section. This difference supports the hypothesis that shading improves water use efficiency.

In the paneled section, ET initially declined sharply with increasing H (0 to ~75 W $m^{-2}$), followed by a steep rise peaking around 145 W $m^{-2}$, and then a moderate decrease. The sunlit section showed a gradual increase in ET with H, peaking around 200 W $m^{-2}$ before leveling off. In the paneled section, higher wind speeds were associated with lower H but not clearly with ET, while no strong correlation was observed in the sunlit section (Figure 2).

The relationship between ET and T also differed between sections. The paneled section showed a nonlinear increase in ET with T, peaking at ~311 K. The sunlit section displayed a more limited ET response and lower rates. Higher VPD values amplified these differences, with the paneled section maintaining higher ET rates under high VPD (Figure 3)."

3.1.4. Seasonal Trends

Comparing summer (higher stress) and autumn (lower stress) in the plum orchard showed clear seasonal effects. During the summer, the paneled area maintained higher $CO_2$ absorption and ET rates compared to the sunlit area, especially as heat stress increased. In autumn, the differences between the paneled and sunlit areas were smaller due to lower overall environmental stress, but none the less the paneled area still generally exhibited better performances. This suggests shading is most beneficial when the weather is hot and dry.

 doi:10.20944/preprints202605.1890.v1



### *3.2. Nectarine Orchard (Yiftah)*

#### 3.2.1. Meteorological Context

Summer daytime VPD was markedly lower beneath the photovoltaic panels than in the adjacent sunlit rows. H showed a similar pattern and was significantly lower in the shaded section compared to the sunlit section. In contrast, neither prevailing wind nor air T differed significantly between treatments.

**Table 4.** Statistical summary of mean, standard deviation, and statistical significance (p-value) for key meteorological variables in the nectarine orchard, comparing paneled and sunlit sections during summer daytime (N=1,136).

| **Meteorological Variable** | **Paneled Section (*Mean* ± *SD*)** | **Sunlit Section (*Mean* ± *SD*)** | ***p*-value** |
|---|---|---|---|
| Vapor-Pressure Deficit (VPD) (Pa) | 2092 ± 520 | 2358 ± 745 | < 0.001 |
| Sensible Heat Flux (H) (W $m^{-2}$) | 88 ± 54 | 101 ± 61 | < 0.001 |
| Prevailing Wind Speed ($u_{rot}$) (m $s^{-1}$) | 2.09 ± 0.80 | 2.04 ± 0.86 | 0.32 |
| Air Temperature (T) (K) | 303.36 ± 2.08 | 303.33 ± 2.68 | 0.84 |

These results indicate that, at this drier orchard, panel shading chiefly moderates atmospheric demand (lower VPD) and surface energy partitioning (lower H) without materially altering mean thermal or wind conditions.

#### 3.2.2. PCA

PCA was conducted on the nectarine orchard data. PC1 showed a strong negative correlation with VPD and T, a negative but less dominant relationship with $u_{rot}$, and a positive relationship with H. PC2 had the strongest negative correlation with $u_{rot}$ and the strongest positive correlation with H, with smaller positive contributions from VPD and T. PC3 was primarily characterized by strong negative correlations with H and $u_{rot}$, a minor negative relationship with VPD, and a very weak positive relationship with T. The first three principal components explained 96.61% of the total variance.

Linear regression models for ET and CO2 flux based on the principal components were significant ($p < 0.001$) during the summer season (July 7th - September 21st) between 8 AM and 5 PM. The models explained 44.95% and 42.76% of the variability in ET and $CO_2$ flux, respectively.

#### 3.2.3. Fluxes (Summer, 8 AM-5 PM)

$CO_2$ flux

$CO_2$ flux measurements during the summer (8 AM - 5 PM) in the nectarine orchard revealed a significant difference between the paneled and sunlit sections, as detailed in Table 5. The paneled section showed consistently higher $CO_2$ absorption, indicating greater photosynthetic activity compared to the sunlit section.

**Table 5.** Statistical summary of mean, standard deviation, and statistical significance (F-statistic, p-value) for $CO_2$ flux and ET in the nectarine orchard, comparing paneled and sunlit sections during summer daytime.

| **Variable** | **Treatment** | ***Mean* ± *SD*** | **Statistical Comparison (*F*-statistic, *p*-value)** |
|---|---|---|---|

 doi:10.20944/preprints202605.1890.v1



| | | | |
|---|---|---|---|
| $CO_2$ flux | Paneled | -15.618 ± 3.946 μmol $m^{-2}$ $s^{-1}$ | $F_{1,1136}$=336.45, p<0.001 |
| | Sunlit | -12.39 ± 4.016 μmol $m^{-2}$ $s^{-1}$ | |
| ET | Paneled | 0.2677 ± 0.0707 mm $hr^{-1}$ | $F_{1,1136}$=195.41, p<0.001 |
| | Sunlit | 0.2549 ± 0.0788 mm $hr^{-1}$ | |

The relationship between $CO_2$ flux and H in the paneled section was more consistent and linear, with $CO_2$ absorption increasing as sensible heat flux increased up to approximately 200 W $m^{-2}$, suggesting a moderated microclimatic response. In contrast, the sunlit section exhibited a broader spread of data points, reflecting greater variability and sensitivity to environmental fluctuations. Wind speed did not show a consistent trend with $CO_2$ flux in either section (Figure 4).

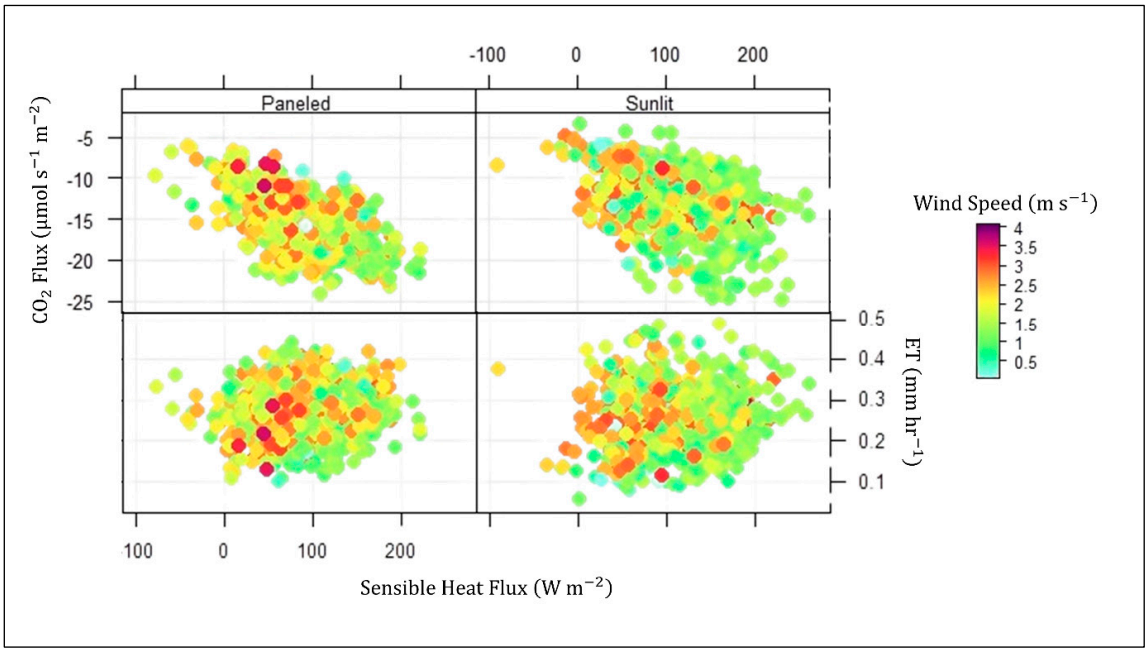


**Figure 4.** Relationship between $CO_2$ flux (top) and evapotranspiration (ET, bottom) versus sensible heat flux in the nectarine orchard. Data are shown for paneled (left) and sunlit (right) sections during summer daytime hours. Data points are colored according to prevailing wind speed.

The relationship between $CO_2$ flux and T in the paneled section displayed variability, with a slight decrease in absorption observed at T above approximately 308 K. The sunlit section showed a more pronounced decrease in $CO_2$ absorption as T rose from about 305 K to 314 K, reflecting its sensitivity to higher T and VPD. Conversely, the paneled section exhibited more moderated responses to T due to shading (Figure 5).

 doi:10.20944/preprints202605.1890.v1



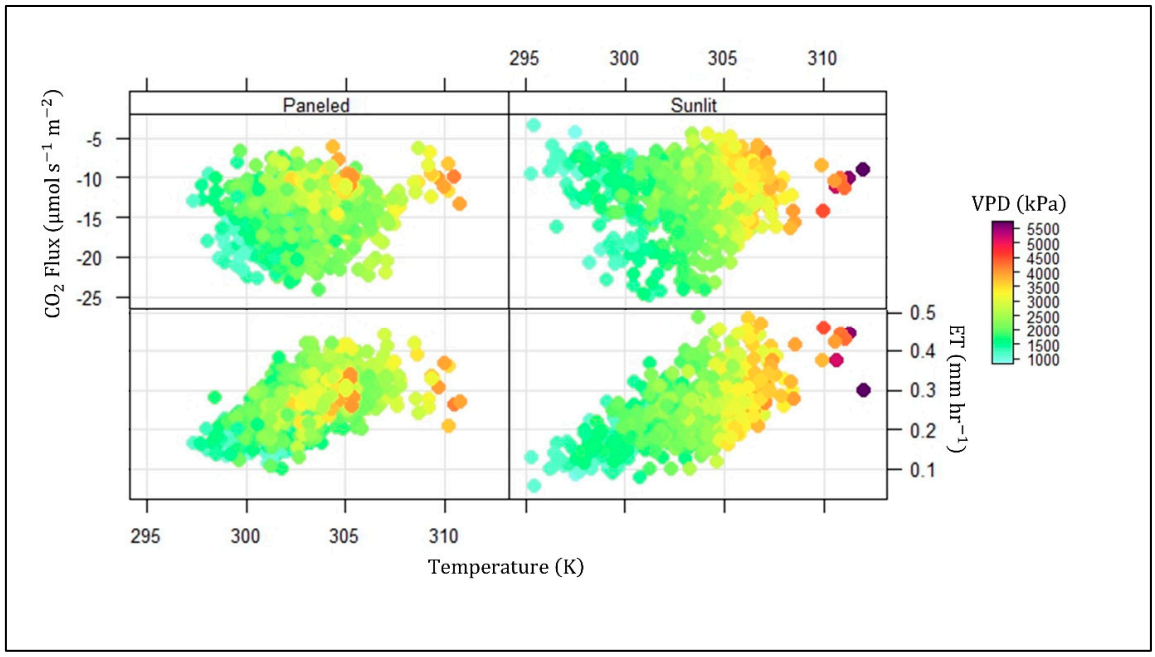


**Figure 5.** Relationship between $CO_2$ flux (top) and evapotranspiration (ET, bottom) versus temperature in the nectarine orchard. Data are shown for paneled (left) and sunlit (right) sections during summer daytime hours. Data points are colored according to vapor pressure deficit (VPD).

Evapotranspiration

ET rates during the summer (8 AM - 5 PM) also showed a small yet statistically significant difference between the paneled and sunlit sections (Table 5). The paneled section had slightly higher mean ET rates compared to the sunlit section.

The relationship between ET and H in the paneled section was nonlinear, showing an initial increase, followed by stabilization, and then a slight decline. The sunlit section exhibited a more gradual increase in ET with H, peaking around 100 W $m^{-2}$ before stabilizing at higher flux levels. Higher wind speeds in the paneled section appeared to correlate with lower sensible heat flux but not clearly with ET, while no strong correlation was evident in the sunlit section (Figure 4).

When examining the relationship between ET and T, the paneled section showed a nonlinear increase, stabilizing around 308 K. The sunlit section, however, exhibited a more linear increase with T without clear stabilization. Higher VPD values appeared to correlate with increased T and ET in both sections (Figure 5).

3.2.4. Seasonal Trends

Seasonal changes in the nectarine orchard also indicated the benefit of shading. During the summer, the paneled section showed more consistent $CO_2$ absorption and ET responses compared to the sunlit area, which was more variable and sensitive to summer heat and dryness. In autumn, as conditions became milder, the differences between the paneled and sunlit sections were reduced, similar to the plum orchard. This reinforces that shading helps buffer the trees against harsh summer conditions.

## 4. Discussion

This study highlights the potential benefits of APV systems in enhancing crop performance under semi-arid conditions. By analyzing the interaction between meteorological variables and plant fluxes, significant differences between the paneled (shaded) and sunlit areas were identified,

 doi:10.20944/preprints202605.1890.v1



demonstrating that the simulated PV-like shading reduced environmental stress and enhanced plant physiological activity.

### *4.1. Key Findings*

The application of PCA proved instrumental in extracting the complex relationships among meteorological variables, such as H, T, VPD, and $u_{rot}$. Even with modest differences in microclimatic variables observed between treatments (such as lower VPD and H in the nectarine orchard compared to the plum orchard), PCA effectively reduced the dimensionality of the dataset while preserving over 95% of the critical variance. This approach simplified the interpretation of flux dynamics and provided a strong statistical basis for identifying treatment specific differences in $CO_2$ flux and ET.

The comparison between the paneled and sunlit sections revealed consistent advantages for the shaded treatments. In the paneled sections of both plum and nectarine orchards, $CO_2$ flux demonstrated significantly higher absorption rates (more negative values) compared to the sunlit sections. This increased carbon assimilation is likely attributable to the moderating effects of shading, which reduced environmental stressors such as excessive heat and high VPD. By mitigating these stresses, shading promoted stomatal opening and enhanced photosynthetic activity, allowing for greater $CO_2$ uptake. Conversely, the sunlit sections exhibited reduced $CO_2$ absorption, with fluxes showing greater sensitivity to rising T and H, suggesting that unshaded conditions amplified stress and likely led to stomatal closure, suppressing carbon assimilation.

Similarly, ET rates were consistently higher in the paneled sections compared to the sunlit sections in both orchards, although the difference was less pronounced than for $CO_2$ flux. The shading provided by the simulated APV systems likely created a more favorable microclimate, enabling sustained transpiration without excessive water loss, thereby contributing to improved water use efficiency. In contrast, the sunlit sections showed lower ET rates and greater sensitivity to combined heat and vapor pressure stress, highlighting the tradeoff between water conservation and gas exchange in unshaded conditions.

Statistical models and visualizations, such as linear regression and scatter plots, were crucial for elucidating these dynamics and treatment specific responses. For instance, the nonlinear response of $CO_2$ flux to T in the paneled sections highlighted the complexity of plant-environment interactions that might otherwise be overlooked in purely statistical analyses. Stratifying the data by variables like wind speed and VPD further added depth to the interpretation, offering a clearer picture of how these relationships varied under different meteorological conditions.

Seasonal variations provided further insights into the adaptability of the treatments. During the summer, when environmental stress was at its peak in Northern Israel, the paneled sections consistently outperformed the sunlit sections in both $CO_2$ absorption and ET rates. This reinforces the hypothesis that shading mitigates stress by creating a buffer against extreme heat and vapor pressure conditions. In autumn, as environmental stress decreased, the differences between the treatments were less pronounced; however, the paneled sections still generally maintained higher flux rates, demonstrating the persistent benefits of shading across seasons.

### *4.2. Site-Specific Responses and Relation to Prior Shading Studies*

The differences in scatterplot trends and the magnitude of microclimatic changes between the plum and nectarine orchards highlight the influence of site-specific factors on micrometeorological responses under simulated APV shading. These variations likely originate from differences in orchard characteristics (tree height, planting density, specific cultivar responses, topography), localized microclimatic conditions, and species-specific physiological adaptations. For example, the plum orchard showed greater sensitivity to H in the sunlit sections, demonstrated a more linear and consistent response, while the nectarine orchard demonstrated a more linear and consistent response in the paneled sections. These differences underscore the complex interactions between plant physiology, shading, and environmental conditions that need to be considered in APV design.

 doi:10.20944/preprints202605.1890.v1



Our findings align with existing shading and netting research (Middleton & McWaters, 2002), which has shown that moderate shade reduces environmental stress on orchard canopies, leading to increased $CO_2$ flux (stronger photosynthetic uptake) and stable ET. Similarly, improved transpiration and enhanced water-use efficiency under shading are consistent with findings in semi-arid agrivoltaics systems (Barron-Gafford et al., 2019; Elamri et al., 2018; Trommsdorff et al., 2021). While those authors focused on herbaceous crops (such as lettuce) rather than orchards, the parallels in reduced thermal load and improved gas exchange are consistent with our results. This study reinforces the broader conclusion that partial shading can reduce stomatal closure and enhance carbon uptake (Marrou et al., 2013b).

To the best of our knowledge, no previous study has combined eddy covariance flux measurements with partial APV-like shading patterns in deciduous orchards, making this work particularly novel in its methodology. Our approach offers an orchard-scale perspective of how shading influences $CO_2$ absorption and ET in real time, moving beyond traditional climatological data or destructive sampling methods often used in prior orchard focused work.

### *4.3. Limitations and Future Work*

One significant limitation of this study was the footprint size of the eddy covariance system, which inherently exceeded treatments area in both study sites. As a result, measurements taken in the shaded area inevitably included contributions from the adjacent sunlit area and from outside the experimental plots. Midday footprint analysis revealed that only 8-30% of the 90% cumulative fetch in the paneled sections intersected the shaded rows, with the point of maximum flux density ($x_{peak}$≈ 8–10 m) falling within the shaded strips. However, beyond this distance, the remaining 70-92% of the cumulative source area covered sunlit canopy. This mixing of footprints means that our reported $CO_2$ and ET differences likely represent conservative lower-bound estimates of the true treatment effect, as the shade signal was diluted by fluxes from unshaded areas. Despite this inherent limitation, the statistical analysis still yielded significant differences between the shaded and unshaded sections, providing valuable evidence of PV-like shading's impact. Future APV studies should prioritize experimental designs that enlarge the shaded treatment areas and ensure the EC tower's footprint lies predominantly within either the shaded or control zones to allow for cleaner flux comparisons.

Another notable limitation of this study was the use of a single EC system, which alternated between the paneled and sunlit sections approximately every 10-15 days. This setup precluded the ability to obtain simultaneous measurements from both sections. Consequently, temporal variations in micrometeorological conditions may have introduced additional variability into the flux measurements, limiting the ability to fully isolate the influence of shading from other temporal factors. Future studies employing two simultaneous EC systems could provide a more robust comparison, enabling clearer insights into the real time dynamics between shaded and sunlit sections.

An additional critical consideration that emerged during this study involves orchard yield. Although our primary focus was micrometeorological measurements, some of the growers expressed concern about potential reductions in fruit yield under partial shading. We did not formally quantify crop production (fruit quantity or quality) within the paneled and sunlit sections, so definitive conclusions about yield impacts cannot be drawn. Nonetheless, the dissatisfaction reported by the agriculturists underscores the importance of rigorously addressing this topic. Future research must incorporate systematic yield assessments, including fruit quantity, quality, and economic returns, while simultaneously quantifying the energy generation obtainable with the APV system. Integrating these diverse data streams will allow for a comprehensive economic evaluation, balancing the potential income from renewable energy with any changes in orchard productivity. Such a holistic approach is essential to fully assess the practicality and long-term benefits of APV systems in commercial orchards.

In summary, future APV research requires the deployment of dual, footprint-matched EC towers, enlarged shaded treatments, and the pairing of flux monitoring with detailed crop yield and

 doi:10.20944/preprints202605.1890.v1



energy generation measurements to comprehensively quantify both the biophysical benefits and economic trade-offs of orchard PV-like shading.

## 5. Conclusions

Our study demonstrates that APV shading can meaningfully influence both $CO_2$ and water vapor fluxes in deciduous orchards under semi-arid conditions. By reducing micrometeorological stressors, partial shading consistently led to more negative $CO_2$ fluxes (higher carbon uptake) and maintained, or slightly elevated, evapotranspiration rates compared to unshaded plots. Although our findings are acknowledged as conservative due to the limited area of the paneled sections, footprint mixing, and the use of a single EC system, they nonetheless provide compelling evidence that shading buffers environmental extremes and promotes physiological conditions favorable to photosynthesis.

From a practical standpoint, these results suggest that integrating solar panels with tree crops may enhance resource use efficiency without necessarily compromising fruit yield, especially in water limited regions. However, the absence of direct yield and energy generation data means that the full agronomic and economic trade-offs remain to be quantified. To translate these biophysical insights into robust management recommendations, future work should pair microclimate flux monitoring with systematic assessments of fruit quantity, quality, and panel output. Such comprehensive evaluations will be essential for determining the overall viability and profitability of APV systems in commercial orchards.

Ultimately, our research lays the groundwork for a more nuanced understanding of how controlled shading affects orchard ecosystems. By demonstrating clear biophysical benefits, even under the methodological constraints identified, we strengthen the case for APV as a dual-use technology that can support both food production and renewable energy goals in water-limited regions.

**Author Contributions: Dafna Eliyahou:** Conceptualization, Software, Validation, Formal analysis, Investigation, Data Curation, Resources, Writing – Original Draft, Writing - Review & Editing, Visualization. **Giora Rytwo:** Conceptualization, Methodology, Validation, Resources, Writing - Review & Editing, Supervision, Project administration, Funding acquisition.

**Funding:** This work was supported by the PRIMA Programme - LENSES project, supported by the European Union [grant number 2041]; the MIGAL-Galilee Research Institute; and Tel-Hai University of Kiryat Shmona.

**Declaration of generative AI and AI-assisted technologies in the writing process**: During the preparation of this work the author(s) used Gemini (Google) in order to review the manuscript for compliance with the journal's guidelines and improve clarity. After using this tool, the author(s) reviewed and edited the content as needed and take(s) full responsibility for the content of the published article.

**Acknowledgements:** The authors thank Prof. Uri Marchaim and the team at MIGAL – Galilee Research Institute Precision Agriculture, and to Dr Moshe Meron, Dr Yitzhak Tsipris and the team at at MIGAL – Galilee Research Institute Agricultural Meteorology for their field assistance and insightful discussions . We also thank Chen Barak for assistance with instrument deployment and sampling, and Sivan Margalit for expert guidance in statistics and coding.

## References

Abdi, H., Williams, L.J., 2010. Principal component analysis. Wiley Interdiscip Rev Comput Stat. https://doi.org/10.1002/wics.101

Allen, R. G., Pereira, L. S., Raes, D., & Smith, M. (1998). *Crop evapotranspiration—Guidelines for computing crop water requirements* (FAO Irrigation and Drainage Paper 56). Rome: FAO. https://www.fao.org/4/x0490e/x0490e00.htm

 doi:10.20944/preprints202605.1890.v1



Aubinet, M., Vesala, T., Papale, D., 2012. Eddy Covariance: A Practical Guide to Measurement and Data Analysis, Springer. Springer Netherlands, Dordrecht, Netherlands. https://doi.org/10.1007/978-94-007-2351-1

Baldocchi, D.D., Law, B.E., Anthoni, P.M., 2000. On measuring and modeling energy fluxes above the floor of a homogeneous and heterogeneous conifer forest. Agric For Meteorol 102, 187–206. https://doi.org/10.1016/S0168-1923(00)00098-8

Barron-Gafford, G.A., Pavao-Zuckerman, M.A., Minor, R.L., Sutter, L.F., Barnett-Moreno, I., Blackett, D.T., Thompson, M., Dimond, K., Gerlak, A.K., Nabhan, G.P., Macknick, J.E., 2019. Agrivoltaics provide mutual benefits across the food–energy–water nexus in drylands. Nature Sustainability 2019 2:9 2, 848–855. https://doi.org/10.1038/s41893-019-0364-5

Beck, M., Bopp, G., Goetzberger, A., Obergfell, T., Reise, C., & Schindele, S. (2012). Combining PV and food crops to agrophotovoltaic—Optimization of orientation and harvest. *Proceedings of the 27th European Photovoltaic Solar Energy Conference and Exhibition (EU PVSEC 2012)*. https://doi.org/10.4229/27thEUPVSEC2012-5AV.2.25

Boote, K. J., & Loomis, R. S. (Eds.). (1991). *Modeling crop photosynthesis—from biochemistry to canopy*. Madison, WI: Crop Science Society of America. doi:10.2135/cssaspecpub19

Burba, G. (2013). *Eddy covariance method for scientific, industrial, agricultural and regulatory applications: A field book on measuring ecosystem gas exchange and areal emission rates*. Lincoln, NE: LI-COR Biosciences. https://www.licor.com/products/eddy-covariance/ec-book

Dinesh, H., Pearce, J.M., 2016. The potential of agrivoltaic systems. Renewable and Sustainable Energy Reviews 54, 299–308. https://doi.org/10.1016/J.RSER.2015.10.024

Dupraz, C., Marrou, H., Talbot, G., Dufour, L., Nogier, A., Ferard, Y., 2011. Combining solar photovoltaic panels and food crops for optimising land use: Towards new agrivoltaic schemes. Renew Energy 36, 2725–2732. https://doi.org/10.1016/j.renene.2011.03.005

Elamri, Y., Cheviron, B., Lopez, J.-M., Dejean, C., Belaud, G., 2018. Water budget and crop modelling for agrivoltaic systems: Application to irrigated lettuces. https://doi.org/10.1016/j.agwat.2018.07.001

U.S. Energy Information Administration. (2016). *International energy outlook 2016: With projections to 2040* (DOE/EIA-0484(2016)). Washington, DC: U.S. Department of Energy. https://www.eia.gov/outlooks/ieo/pdf/0484(2016).pdf

European Commission. (2011). A roadmap for moving to a competitive low carbon economy in 2050 (COM(2011) 112 final). Brussels: European Commission. https://eur-lex.europa.eu/LexUriServ/LexUriServ.do?uri=COM:2011:0112:FIN:EN:PDF

Farquhar, G. D., Lloyd, J., Taylor, J. A., Flanagan, L. B., Syvertsen, J. P., Hubick, K. T., Wong, S. C., & Ehleringer, J. R. (1993). Vegetation effects on the isotope composition of oxygen in atmospheric $CO_2$. *Nature, 363*(6428), 439–443. https://doi.org/10.1038/363439a0

Foken, T., Aubinet, M., Leuning, R., 2012. The Eddy Covariance Method, in: Eddy Covariance. Springer Netherlands, pp. 1–19. https://doi.org/10.1007/978-94-007-2351-1_1

Foley, J.A., Kutzbach, J.E., Coe, M.T., Levis, S., 1994. Feedbacks between climate and boreal forests during the Holocene epoch.

Gates, D.M., 1968. Transpiration and leaf temperature. Annu Rev Plant Physiol 19, 211–238.

Glenn, D. M. (2009). Particle film mechanisms of action that reduce the effect of environmental stress in 'Empire' apple. *Journal of the American Society for Horticultural Science, 134*(3), 314–321. https://doi.org/10.21273/JASHS.134.3.314

Goetzberger, A., Zastrow, A., 1982. On the Coexistence of Solar-Energy Conversion and Plant Cultivation. International Journal of Solar Energy 1, 55–69. https://doi.org/10.1080/01425918208909875

Grappadelli, L.C., Lakso, A.N., Flore, J.A., 1994. Early season patterns of carbohydrate partitioning in exposed and shaded apple branches. J. Am. Soc. Hortic. Sci 119, 596–603.

Gu, L., Massman, W.J., Leuning, R., Pallardy, S.G., Meyers, T., Hanson, P.J., Riggs, J.S., Hosman, K.P., Yang, B., 2012. The fundamental equation of eddy covariance and its application in flux measurements. Agricultural and Forest Meteorology. 152: 135-148. 152, 135–148. https://doi.org/10.1016/J.AGRFORMET.2011.09.014

 doi:10.20944/preprints202605.1890.v1



Hassanpour, E., Id, A., Selker, J.S., Higgins, C.W., 2018. Remarkable agrivoltaic influence on soil moisture, micrometeorology and water-use efficiency. https://doi.org/10.1371/journal.pone.0203256

Hubbard, K. G., & Hollinger, S. E. (2005). Standard meteorological measurements. In J. L. Hatfield & J. M. Baker (Eds.), *Micrometeorology in agricultural systems* (Agronomy Monograph No. 47, pp. 1–30). Madison, WI: ASA–CSSA–SSSA. https://doi.org/10.2134/agronmonogr47.c1

International Renewable Energy Agency (IRENA). (2019). *Renewable power generation costs in 2018*. Abu Dhabi: IRENA. https://www.irena.org/publications/2019/May/Renewable-power-generation-costs-in-2018

International Renewable Energy Agency (IRENA). (2023). *Renewable power generation costs in 2022*. Abu Dhabi: IRENA. https://www.irena.org/-/media/Files/IRENA/Agency/Publication/2023/Aug/IRENA_Renewable_power_generation_costs_in_2022.pdf

Jarvis, P.G., 1976. The interpretation of the variations in leaf water potential and stomatal conductance found in canopies in the field. Philosophical Transactions of the Royal Society of London. B, Biological Sciences 273, 593–610. https://doi.org/10.1098/RSTB.1976.0035

Jolliffe, I. T. (2002). Principal component analysis for special types of data. In *Principal component analysis* (2nd ed., pp. 338–372). New York, NY: Springer. https://doi.org/10.1007/0-387-22440-8_13

Kramer, P. J., & Boyer, J. S. (1995). *Water relations of plants and soils*. San Diego, CA: Academic Press. https://shop.elsevier.com/books/water-relations-of-plants-and-soils/kramer/978-0-12-425060-4

Lehner, M., Rotach, M.W., 2018. Current challenges in understanding and predicting transport and exchange in the atmosphere over mountainous terrain. Atmosphere (Basel). https://doi.org/10.3390/atmos9070276

Lewis, N.S., Nocera, D.G., 2006. Powering the planet: Chemical challenges in solar energy utilization. Proc Natl Acad Sci U S A 103, 15729–15735. https://doi.org/10.1073/PNAS.0603395103

Mahrer, Y., Rytwo, G., 1991. Modelling and measuring evapotranspiration in a daily drip irrigated cotton field. Irrig Sci 12, 13–20. https://doi.org/10.1007/BF00190704

Marrou, H., Dufour, L., Wery, J., 2013a. How does a shelter of solar panels influence water flows in a soil-crop system? European Journal of Agronomy 50, 38–51. https://doi.org/10.1016/j.eja.2013.05.004

Marrou, H, Guilioni, L., Dufour, L., Dupraz, C., Wery, J., 2013b. Microclimate under agrivoltaic systems: Is crop growth rate affected in the partial shade of solar panels? Agric For Meteorol 177, 117–132. https://doi.org/10.1016/j.agrformet.2013.04.012

Middleton, S., & McWaters, A. (2002). Hail netting of apple orchards—Australian experience. *Compact Fruit Tree, 35*(2), 51–55. https://era.dpi.qld.gov.au/id/eprint/8117/1/10.1.1.550.1282.pdf

Nonhebel, S., 2005. Renewable energy and food supply: Will there be enough land? Renewable and Sustainable Energy Reviews 9, 191–201. https://doi.org/10.1016/J.RSER.2004.02.003

Preisendorfer R. W., 1988. Principal Component Analysis in Meteorology and Oceanography. Elsevier, Amsterdam.

Prentice, I.C., Heimann, M., Sitch, S., 2000. The Carbon Balance Of The Terrestrial Biosphere: Ecosystem Models And Atmospheric Observations. Ecological Applications 10, 1553–1573.

Ravi, S., Macknick, J., Lobell, D., Field, C., Ganesan, K., Jain, R., Elchinger, M., Stoltenberg, B., 2016. Colocation opportunities for large solar infrastructures and agriculture in drylands. Appl Energy 165, 383–392. https://doi.org/10.1016/J.APENERGY.2015.12.078

Rogner, H.-H., Aguilera, R. F., Archer, C. L., Bertani, R., Bhattacharya, S. C., Dusseault, M. B., Gagnon, L., Haberl, H., Hoogwijk, M., Johnson, A., Rogner, M. L., Wagner, H., & Yakushev, V. (2012). Energy resources and potentials. In *Global energy assessment: Toward a sustainable future* (pp. 425–512). Cambridge, UK and New York, NY, USA: Cambridge University Press; Laxenburg, Austria: IIASA. https://www.cambridge.org/core/books/global-energy-assessment/energy-resources-and-potentials/27BD5732DE9C9A57B662AC3724580468

Rytwo, G., Eliyahou, D., 2023. Eddy correlation measurements to visualize CO2 and water vapor concentrations and fluxes. Journal of Agrometeorology 25, 239–246. https://doi.org/10.54386/jam.v25i2.2103

Seidlova, L., Verlinden, A.M., Gloser, A.J., Milbau, A.A., Nijs, A.I., 2009. Which plant traits promote growth in the low-light regimes of vegetation gaps? Plant Ecol 303–318. https://doi.org/10.1007/s11258-008-9454-6

 doi:10.20944/preprints202605.1890.v1



Sellers, P.J., Dickinson, R.E., Randall, D.A., Betts, A.K., Hall, F.G., 1997. Modeling the Exchanges of Energy, Water, and Carbon Between Continents and the Atmosphere. Science (1979) 275, 502–509.

Steiner, J.L., Hatfield, J.L., 2008. Winds of change: A century of agroclimate research. Agron J. https://doi.org/10.2134/agronj2006.0372c

Teixeira, M.A.C., Kirshbaum, D.J., Ólafsson, H., Sheridan, P.F., Stiperski, I., 2016. Editorial: The atmosphere over mountainous regions. Front Earth Sci (Lausanne). https://doi.org/10.3389/feart.2016.00084

Testi, L., Villalobos, F.J., Orgaz, F., 2004. Evapotranspiration of a young irrigated olive orchard in southern Spain. Agric For Meteorol 121, 1–18. https://doi.org/10.1016/J.AGRFORMET.2003.08.005

Tilman, D., Balzer, C., Hill, J., Befort, B., 2011. How to Feed the World in 2050. Science (1979) 327, 812–818. https://doi.org/10.1126/science.1185383

Trommsdorff, M., Kang, J., Reise, C., Schindele, S., Bopp, G., Ehmann, A., Weselek, A., Högy, P., Obergfell, T., 2021. Combining food and energy production: Design of an agrivoltaic system applied in arable and vegetable farming in Germany. Renewable and Sustainable Energy Reviews 140. https://doi.org/10.1016/j.rser.2020.110694

United Nations Convention to Combat Desertification (UNCCD). (2017). *Global Land Outlook: First edition*. Bonn, Germany: UNCCD. https://web.archive.org/web/20170926020043/http://archive.unccd.int/download/GLO_Full_Report_hi_res.pdf

United Nations, Department of Economic and Social Affairs, Population Division. (2021). *Global population growth and sustainable development*. New York: United Nations. https://www.un.org/development/desa/pd/sites/www.un.org.development.desa.pd/files/undesa_pd_2022_global_population_growth.pdf

United Nations Framework Convention on Climate Change (UNFCCC). (2015). *Adoption of the Paris Agreement* (FCCC/CP/2015/L.9/Rev.1). Paris: UNFCCC. https://unfccc.int/resource/docs/2015/cop21/eng/l09r01.pdf

Valle, B., Simonneau, T., Sourd, F., Pechier, P., Hamard, P., Frisson, T., Ryckewaert, M., Christophe, A., 2017. Increasing the total productivity of a land by combining mobile photovoltaic panels and food crops. Appl Energy 206, 1495–1507. https://doi.org/10.1016/J.APENERGY.2017.09.113

Venkatram, A., Schulte, N., 2018. Fundamentals of Micrometeorology and Dispersion, in: Urban Transportation and Air Pollution. Elsevier, pp. 39–75. https://doi.org/10.1016/b978-0-12-811506-0.00003-8

Weselek, A., Bauerle, A., Hartung, J., Zikeli, S., Lewandowski, I., Högy, P., 2021. Agrivoltaic system impacts on microclimate and yield of different crops within an organic crop rotation in a temperate climate. Agron Sustain Dev 41, 59. https://doi.org/https://doi.org/10.1007/s13593-021-00714-y

Wold, S., Esbensen, K., & Geladi, P. (1987). Principal component analysis. *Chemometrics and Intelligent Laboratory Systems, 2*(1–3), 37–52. https://doi.org/10.1016/0169-7439(87)80084-9